NeuroImage 220 (2020) 117074

Contents lists available at ScienceDirect

NeuroImage

journal homepage: www.elsevier.com/locate/neuroimage

A gradient from long-term memory to novel cognition: Transitions through default mode and executive cortex

Xiuyi Wang [a,*], Daniel S. Margulies [b], Jonathan Smallwood [a], Elizabeth Jefferies [a,**]

[a] Department of Psychology, University of York, Heslington, York, YO10 5DD, United Kingdom
[b] Centre National de la Recherche Scientifique (CNRS) UMR 7225, Frontlab, Institut du Cerveau et de la Moelle Épinière, Paris, France

ARTICLE INFO

Keywords:
Semantic
Gradient
Default mode network
Semantic control
Multiple demand network

ABSTRACT

Human cognition flexibly guides decision-making in familiar and novel situations. Although these decisions are often treated as dichotomous, in reality, situations are neither completely familiar, nor entirely new. Contemporary accounts of brain organization suggest that neural function is organized along a connectivity gradient from unimodal regions of sensorimotor cortex, through executive regions to transmodal default mode network. We examined whether this graded view of neural organization helps to explain how decision-making changes across situations that vary in their alignment with long-term knowledge. We used a semantic judgment task, which parametrically varied the global semantic similarity of items within a feature matching task to create a 'task gradient', from conceptual combinations that were highly overlapping in long-term memory to trials that only shared the goal-relevant feature. We found the brain's response to the task gradient varied systematically along the connectivity gradient, with the strongest response in default mode network when the probe and target items were highly overlapping conceptually. This graded functional change was seen in multiple brain regions and within individual brains, and was not readily explained by task difficulty. Moreover, the gradient captured the spatial layout of networks involved in semantic processing, providing an organizational principle for controlled semantic cognition across the cortex. In this way, the cortex is organized to support semantic decision-making in both highly familiar and less familiar situations.

1. Introduction

Cognition supports behavioural flexibility by guiding decision-making in a manner that is appropriate to our changing circumstances. Although long-term knowledge can support our decisions in familiar situations, in novel circumstances, knowledge is not available to constrain our choices (Kahneman, 2003; Tversky and Kahneman, 1974). Traditionally, these different facets of cognition have been ascribed to dichotomous neural systems. Regions within the lateral anterior temporal lobe and angular gyrus, allied to the default mode network (DMN), are assumed to play a role when the knowledge required by a task is readily available within long-term memory (Badre and Wagner, 2007; Bemis and Pylkkänen, 2013; Davey et al., 2016; Humphreys and Lambon Ralph, 2015, 2017; Lau et al., 2013; Teige et al., 2018; Wagner et al., 2001). In the absence of long-term knowledge, decisions are supported by the multiple demand network (MDN), including the inferior frontal sulcus, intraparietal sulcus, and pre-supplementary motor area, which support short-term goals in working memory (Duncan, 2010; Fedorenko et al., 2013).

Although familiar and novel situations are often treated as dichotomous, many everyday contexts are neither completely familiar, nor entirely novel. This is highlighted by the domain of semantic cognition: semantic retrieval is reliant on knowledge stored within long-term memory – yet the conceptual store in isolation is not sufficient for successful semantic performance (Jefferies, 2013; Lambon Ralph et al., 2017). This is because we have learned about many features and associations for any given concept, yet only a subset of this knowledge will be relevant at any given moment. To generate flexible and more novel patterns of retrieval appropriate to specific tasks and contexts, control processes are thought to interact with our store of conceptual knowledge (Chiou et al., 2018; Davey et al., 2016). This raises the question of how functional responses within DMN and MDN may change within semantic tasks, depending on the extent to which meaningful inputs are fully coherent with the structure of knowledge in long-term memory or

* Corresponding author.
** Corresponding author.
E-mail addresses: xiuyi.wang@york.ac.uk, wangxiuyi16@gmail.com (X. Wang), beth.jefferies@york.ac.uk (E. Jefferies).

https://doi.org/10.1016/j.neuroimage.2020.117074
Received 2 March 2020; Received in revised form 21 May 2020; Accepted 17 June 2020
Available online 20 June 2020

instead require a more novel pattern of retrieval to be generated that can highlight task-specific features.

Contemporary accounts of cortical organization suggest that intrinsic connectivity and functional organization may change gradually and systematically along the cortical surface (Margulies et al., 2016). Margulies et al. (2016) described the principal gradient of the human brain, recovered through diffusion embedding techniques that decompose variance in connectivity into its spatial components. A gradient is a whole brain pattern corresponding to one of these components which captures the systematic change in functional connectivity along the cortical surface. Areas would occupy similar positions along the gradient if they resemble each other with respect to the connectivity component of interest. It was found that neural systems are organized along a gradient that extends from primary sensorimotor areas at one end, through attention and executive areas of MDN, to transmodal DMN regions at the opposite end (Margulies et al., 2016). This organizational property of the cortex is reflected in its geometry, with the DMN located in regions of cortex that are physically most distant (in millimeter) from sensory-motor systems. Since there are multiple DMN peaks in the brain, there are multiple spatial gradients (or 'zones') extending along the cortical surface from the DMN – with similar patterns within temporal, medial and lateral prefrontal cortex (Badre and Nee, 2018; Huntenburg et al., 2018; Jackson et al., 2019; Margulies et al., 2016; Nee and D'Esposito, 2016; Lambon Ralph et al., 2017). In this way, the macroscale organization of the cortex highlighted by the principal connectivity gradient offers a view of neural organization in which the relationships between systems are graded rather than dichotomous, with transitions between networks in multiple cortical zones following the same orderly sequence.

Motivated by this novel view of how neural function is organized, the current study examines whether this cortical gradient of connectivity (Margulies et al., 2016) reflects how semantic decisions change in a graded fashion as the support from heteromodal long-term knowledge is varied. Hub and spoke accounts of semantic representation suggest that semantic cognition emerges from interactions of representations situated at different points along this gradient – including both a heteromodal hub in anterior parts of the temporal lobe, and visual and auditory spoke regions in posterior and superior portions of the temporal lobe respectively (Lambon Ralph et al., 2017). Heteromodal concepts are thought to emerge from the convergence of different sensory-motor features in a relatively graded fashion (Lambon Ralph et al., 2017), creating a unimodal to heteromodal gradient within ventrolateral temporal that is reminiscent of the principal gradient. At the heteromodal end of this gradient, long-term conceptual knowledge captures multiple partially-overlapping shared features between similar items drawn from the same taxonomic category, while at the unimodal end, specific features might be represented in the absence of conceptual similarity (Chiou et al., 2018). We therefore created an experimental paradigm in which participants decided whether concepts shared a specific feature (such as colour), whilst varying their overall semantic similarity. Participants were asked to decide if two words, presented successively, overlapped in colour, shape or size. We varied the number of other features that the two items shared parametrically, creating a spectrum of trials ranging from situations in which only the goal-relevant feature was shared (e.g., colour: tomato and lipstick) to trials in which nearly all features were shared (e.g., colour: strawberry and raspberry). We measured neural activity in thirty participants using functional magnetic resonance imaging (fMRI) to establish the correspondence between the connectivity gradient described by Margulies et al. (2016) and our 'task gradient' – i.e., changes in the neural response to the feature-matching task as the semantic similarity varied. Trials with more shared features are expected to generate stronger responses in regions of the DMN (given the alignment between the task and strongly-encoded information in long-term memory in these circumstances), while concepts that are less globally-overlapping are expected to produce stronger responses in MDN and sensorimotor regions (since participants need to focus on these specific features, represented at the unimodal end of the connectivity gradient, on these trials). In order to be able to independently describe DMN and MDN for each participant, we used well-established localizer paradigms that manipulated the difficulty of cognitive tasks in an independent session. We also recorded resting-state data (rs-fMRI) allowing us to extract the principal connectivity gradient for each participant. In this way, we were able to test whether networks implicated in semantic cognition are organized in a systematic way along the connectivity and task gradients extracted for each individual.

2. Materials and methods

2.1. Participants

The research was approved by local ethics committees and volunteers provided written informed consent. 31 healthy adults were recruited from the University of York (26 females; age: mean ± SD = 20.60 ± 1.68). All participants were right-handed, native English speakers, with normal or corrected-to-normal vision and no history of psychiatric or neurological illness. We excluded one participant who attended only one of two sessions and two runs of one participant and one run of one participant because accuracy was not higher than chance.

2.2. Design and tasks

Participants matched probe and target concepts (presented as written words) according to colour, shape or size, in a rapid event-related design. The goal feature was specified at the start of each trial. The degree of feature overlap between the probe and target was parametrically manipulated: in some trials, the items shared many features (e.g., STRAWBERRY and RASPBERRY), while others only shared the task-relevant feature (e.g. colour match: TOMATO and LIPSTICK) (Fig. 1). Localizer tasks were presented in a different session to define functional networks of interest (Fig. 2). We compared visually-presented words and nonwords to identify sites sensitive to meaning. We also contrasted easy and hard spatial working memory and math decisions to define DMN and MDN (Fedorenko et al., 2013, 2011). Resting-state data was collected to capture the macroscale properties of the cortex. During the scan, participants were instructed to passively view a fixation cross for 9 min and not to think of anything in particular.

2.2.1. Semantic feature matching task

Participants were asked to match probe and target concepts (presented as words) according to a particular semantic feature (colour, shape or size), specified at the start of each trial. We parametrically manipulated the global feature overlap between the probe and target concepts, creating a "task gradient", using semantic similarity ratings taken from a separate group of 30 participants on a 5-point Likert Scale. For example, in colour-matching, STRAWBERRY – RSAPBERRY share many features (not just colour), while TOMATO – LIPSTICK share few features besides colour. The global similarity ratings of the selected trials were evenly distributed from 1 to 5. This parametric design allowed us to model the effect of global feature similarity in the neural data, and test for systematic changes in cortical recruitment along the connectivity gradient defined by Margulies et al. (2016), as semantic similarity increased. Participants were also required to detect non-matches (presented on one third of the trials), which could either be globally-related or unrelated. For example, LEMON and LIME share many features but not colour, while BANANA and RUBY share almost no features, including colour. This ensured that participants had to pay attention to the target feature on each trial. Participants pressed a button with their right index finger to indicate a matching trial, and responded with their right middle finger to indicate a non-matching trial. We then computed behavioural efficiency scores across participants for each item, combining response time (RT) with accuracy: i.e., the mean RT for correct responses across participants was divided by the proportion of correct responses for that item

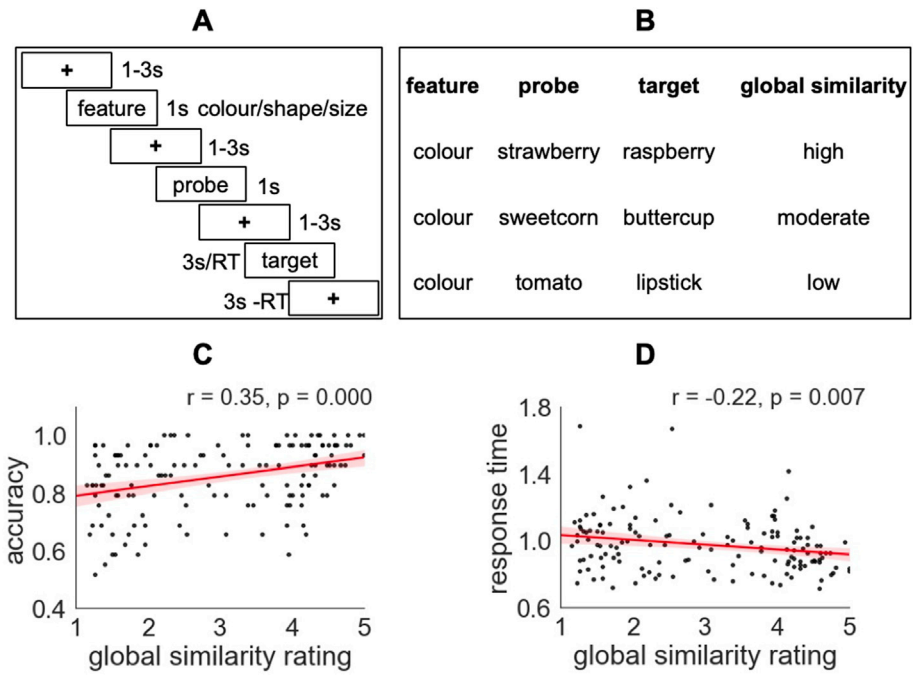

Fig. 1. A – Semantic task structure: first, the feature to be matched was specified (e.g. colour), then the probe word was presented (e.g. strawberry), followed by the target word (e.g. raspberry). Participants indicated if the probe and target shared the specified feature. B – Parametric manipulation of global semantic similarity of matching trials within a semantic feature matching task. We created a 'task gradient' varying from strong to weak alignment between the inputs and long-term memory. C and D show correlations between ratings of global semantic similarity and average performance across 30 participants (each trial is shown as a data point).

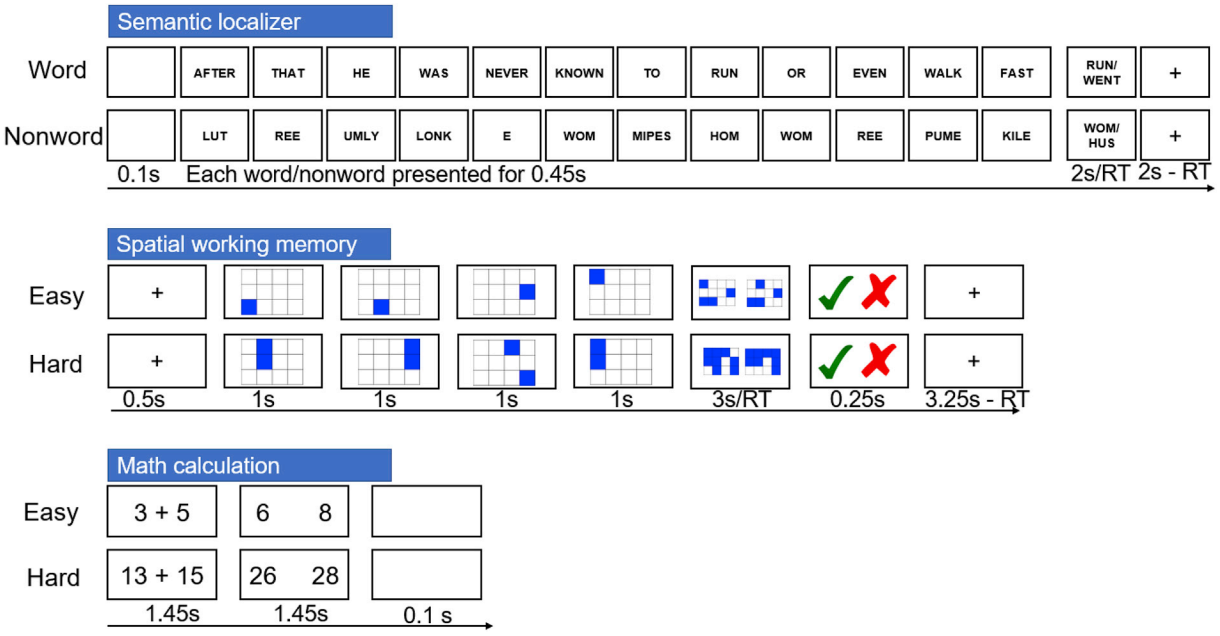

Fig. 2. Illustration of localizer tasks.

(Snodgrass et al., 1985).

In order to maximize the statistical power of the rapid event-related fMRI data analysis, the stimuli were presented with a temporal jitter, randomized from trial to trial (Dale, 1999). The inter-stimulus intervals (between instruction and probe, and probe and target) and the inter-trial interval varied from 1 to 3s. Each trial started with a fixation, followed by a task instruction slide specifying the feature to match (colour, shape or size), presented for 1s. This was followed by the second fixation and then the probe word, presented for 1s. Finally, there was the third fixation followed by the target word, triggering the onset of the decision-making period. The target remained visible until the participant responded, or for a maximum of 3s. The instruction, probe and target words were presented centrally on the screen.

There were 216 trials in total, presented in 4 runs of 54 trials each. Each run lasted for 600s. Global feature similarity was evenly distributed in each run. Within each run, there were 18 trials for each feature. 12 of these 18 trials were matching trials in which probe and target shared the relevant feature, while 6 were non-matching trials. The order of runs and trials within each run was randomized across subjects. The stimuli were presented using Psychopy (Peirce, 2007).

2.2.2. *Localizer tasks*

Localizer tasks were used to define DMN, MDN and semantic regions (adapted from Fedorenko et al., 2011). These tasks are shown in Fig. 2. MDN regions were defined using contrasts of hard over easy spatial working memory or arithmetic judgements, while DMN regions were

defined using the reverse contrasts. The contrast between these conditions has been shown to reveal DMN (easy > hard) and MDN (hard > easy) (Fedorenko et al., 2011). Each localizer task included two runs and two conditions, presented in a standard block design. Condition order was counterbalanced across runs and run order was counterbalanced across participants for each task.

2.2.2.1. Spatial working memory task. Participants had to keep track of four or eight sequentially presented locations in a 3 × 4 grid (Fedorenko et al., 2011), giving rise to easy and hard spatial working memory conditions. Stimuli were presented at the centre of the screen across four steps. Each of these steps lasted for 1s and highlighted one location on the grid in the easy condition, and two locations in the hard condition. This was followed by a decision phase, which showed two grids side by side. One grid contained the locations shown on the previous four steps, while the other contained one or two locations in the wrong place. Participants indicated their recognition of these locations in a two-alternative, forced-choice paradigm via a button press and feedback was immediately provided. Each run consisted 12 experimental blocks (6 blocks per condition and 4 trials in a 32 s block) and 4 fixation blocks (each 16s long), resulting in a total time of 448s.

2.2.2.2. Math task. Participants saw an arithmetic addition expression on the screen for 1.45s and were then given two numbers as choices. The easy condition included smaller single-digit numbers while the hard condition included larger two-digit numbers, also presented for 1.45s. Each trial ended with a blank screen lasting for 0.1s. Each run consisted of 12 experimental blocks (with 4 trials per block) and 4 fixation blocks, resulting in a total time of 316s. In the easy condition, participants use long-term knowledge to decide whether 3 + 5 = 6 or 8. In the hard condition, long-term knowledge is also required to decide whether 13 + 15 = 26 or 28 but this condition places a greater load on working memory and computation and consequently the contrast between these conditions has been shown to reveal DMN and MDN (Fedorenko et al., 2013).

2.2.2.3. Semantic localizer task. Participants read sentences and lists of pronounceable nonwords, followed by a probe recognition test (present/absent judgment for single word and nonword). Sentences contrasted with nonwords reliably activate semantic and language regions (Fedorenko et al., 2016, 2011; 2010; Mahowald and Fedorenko, 2016). Each trial started with a 100 ms blank screen. Stimuli were presented at the centre of the screen, one word/nonword at a time, at the rate of 450 ms per item. The sequence was followed by a probe word/nonword; participants had 2s to decide whether this item had been presented in the sequence, giving a total trial duration of 7.5s. Each run included 16 experimental blocks with 3 trials per block and 5 fixation blocks lasting for 14s. Each run lasted a total of 430s.

Given that the sentences were easier to maintain than the nonwords, the semantic localizer was able to reveal regions involved in semantic processing (including semantically-relevant regions within DMN and potentially also semantic regions responding to control demands outside DMN). However, this localizer contrast is likely to miss MDN regions, which are expected to respond to the difficulty of the nonword condition but might nevertheless contribute to demanding semantic tasks. Consequently, we defined an additional semantic control mask using a meta-analysis of task contrasts in which semantic control demands were manipulated (Noonan et al., 2013). This semantic control map might be expected to overlap with the semantic localizer in control regions specific to semantic processing outside the MDN, as well as other control regions within the MDN.

2.3. MRI data acquisition

Structural and functional data were collected on a Siemens Prisma 3T MRI scanner at the York Neuroimaging Centre. The scanning protocols included a T1-weighted MPRAGE sequence with whole-brain coverage. The structural scan used: acquisition matrix of 176 × 256 × 256 and voxel size 1 × 1 × 1 mm^3, repetition time (TR) = 2300 ms, and echo time (TE) = 2.26 ms. Functional data were acquired using an EPI sequence with a 80^0 flip angle and using GRAPPA with an acceleration factor of 2 in 3 × 3 x 4-mm voxels in 64-axial slices. The functional scan used: 55 3-mm-thick slices acquired in an interleaved order (with 33% distance factor), TR = 3000 ms, TE = 15 ms, FoV = 192 mm.

2.4. MRI data pre-processing

2.4.1. Task fMRI data pre-processing

Pre-processing was carried out using FMRIB's Software Library (FSL version 6, fsl.fmrib.ox.ac.uk/fsl/fslwiki/FEAT/). The T1-weighted structural brain images were extracted. Structural images were registered to the MNI-152 template using FMRIB's linear image registration tool (FLIRT). Task fMRI data pre-processing included motion correction, slice-timing correction, spatial smoothing with a 5 mm FWHM Gaussian filter and high-pass filtering at 100s. Motion-affected volumes were removed from the fMRI data using scrubbing (Power et al., 2012).

2.4.2. Resting-state data pre-processing

Resting-state fMRI data pre-processing was performed using SPM12 (http://www.fil.ion.ucl.ac.uk/spm) and the CONN toolbox (v.18b) (https://www.nitrc.org/projects/conn) (Whitfield-Gabrieli and Nieto-Castanon, 2012), implemented in MATLAB (R2019a) (https://uk.mathworks.com/products/matlab). Pre-processing steps followed CONN's default pipeline which included motion correction, slice-time correction, and simultaneous grey matter (GM), white matter (WM) and cerebrospinal fluid (CSF) segmentation and normalisation to MNI152 stereotactic space (2 mm isotropic) of both functional and structural data. Following pre-processing, the following potential confounders were statistically controlled for: 6 motion parameters and their 1st and 2nd order derivatives, volumes with excessive movement (motion greater than 0.5 mm and global signal changes larger than z = 3), linear drifts, and five principal components of the signal from WM and CSF (CompCor approach) (Behzadi et al., 2007). Finally, data were band-pass filtered between 0.01 and 0.1 Hz. No global signal regression was performed. The pre-processing steps reported here are identical to the ones described in Karapanagiotidis et al. (2019).

2.5. MRI analysis

2.5.1. Parametric task gradient analysis

To examine how the semantic featural overlap is reflected in the strength of the neural response, the parametric modulation of semantic featural overlap was modelled by including a parametric regressor for correct matching trials in the general linear model (GLM). This parametric effect, corresponding to the "task gradient", was modelled using the demeaned global semantic similarity ratings (see section 2.2.1). In addition to this parametric regressor, we also included the main effect of task, which is analogous to the need to include an intercept term in a linear regression model along with the slope term. Demeaned global similarity ratings and the main effect of task were modelled as epochs lasting from the target onset to response, thus controlling for lengthened BOLD responses on trials with longer response times. We also modelled the instruction period, two inter-stimulus interval periods, probe presentation, mismatch trials in which probe and target did not share the specified feature, and incorrect trials as regressors of no interest. We included both of the within-trial inter-stimulus interval periods as regressors of no interest (removing them from the implicit baseline) since participants were maintaining feature information and probe information during these two periods. We also ran the GLM without these two inter-stimulus intervals and the results were largely unchanged. Six head motion parameters were further included in each GLM as regressors of no

interest to control for potential confounding effects of head motion.

2.5.2. Whole-brain functional connectivity gradients

To examine the correspondence between the task gradient and connectivity gradient, we performed dimension reduction analysis on resting state data. Firstly, the functional time-series from 400 regions of interest (ROIs) were extracted for each individual using the Schaefer parcellation (Schaefer et al., 2018). Pearson correlation was calculated to construct a 400 × 400 connectivity matrix for each participant. These individual connectivity matrices were then averaged to calculate a group-averaged connectivity matrix. The Brainspace Toolbox (Vos de Wael et al., 2020) was used to extract ten group-level gradients from the group-averaged connectivity matrix (dimension reduction technique = diffusion embedding, kernel = normalized angle, sparsity = 0.9). Ten gradients were chosen based on the scree plot. These group-level gradient solutions were aligned using Procrustes rotation to a subsample of the HCP dataset ([n = 217, 122 women, mean + sd age = 28.5 + 3.7 y]); for full details of subject selection see Vos De Wael et al. (2018) openly available within the Brainspace toolbox (Vos de Wael et al., 2020).

Using identical parameters, individual-level gradients were then calculated for each individual using their 400 × 400 connectivity matrix. These individual-level gradient maps were aligned to the group-level gradient maps using Procrustes rotation to improve comparison between the group-level gradients and individual-level gradients (N iterations = 10). This analysis resulted in ten group-level gradients and ten individual-level gradients for each participant explaining maximal whole-brain connectivity variance in descending order. The gradient within our sample that showed the greatest correspondence to the principal gradient described by Margulies et al. (2016) was also the component that explained the most variance, capturing the separation between heteromodal and unimodal regions. To compare our connectivity gradient with connectivity gradient revealed by Margulies et al. (2016), we extracted the gradient values of the 400 ROIs respectively, and then performed Pearson correlation across these ROIs. The results are shown in Supplementary Materials Figure S6.

2.5.3. Correlations between task and connectivity gradient at the group level

We examined the spatial correspondence of the connectivity gradient defined by Margulies et al. (2016) and the task gradient for matching trials by computing correlations across voxels in the whole brain and within semantic regions defined using a meta-analytic mask for the term "semantic" from Neurosynth (Yarkoni et al., 2011). To establish whether systematic functional change along the connectivity gradient was seen in multiple cortical areas linked to semantic processing, we also examined the correlations between the task and connectivity gradients using anatomical masks in lateral frontal, medial frontal, temporal and parietal areas (details in Supplementary Materials). We permuted the connectivity gradient values (10000 iterations) to examine whether the correlation coefficients were significantly greater than zero.

2.5.4. Mixed effects modelling

To examine the shape of gradient transitions within the semantic mask from Neurosynth (Yarkoni et al., 2011), voxels were assigned into ten decile bins according to their values on the connectivity gradient (Margulies et al., 2016). We investigated whether there was a linear (or more complex) relationship between the effect of the task manipulation and the connectivity gradient bin within a linear mixed effect model. Parameter estimates for the effect of global feature similarity were extracted from each bin, for each subject and in each run separately, with the model capturing the hierarchical structure of this data. To allow for individual differences in the effect of the gradient and in the overall BOLD response, we allowed for random intercepts and slopes within the model. We compared a model that only included a linear effect of gradient bin with more complex models, such as models that additionally included quadratic and cubic effects. Further details including fit statistics and parameter estimates are provided in Supplementary Materials.

2.5.5. Correlations between gradient values and effects of semantic similarity within individuals

We extracted the parametric effect of the task gradient for matching trials in each voxel and each individual participant to establish how many participants showed a significant correlation between the task gradient and the connectivity gradient. We tested these correlations in each participant within the semantic mask and for each anatomical region of interest. We also permuted the connectivity gradient values (10000 iterations) to examine whether the correlation coefficients were significantly greater than zero.

2.5.6. Localizer task analysis

For the semantic localizer task, we examined the contrast of words with pronounceable nonword task blocks. In the spatial working memory task and math task, we examined the contrast of hard versus easy conditions to define MDN regions, and the reverse to define DMN regions. A grey matter mask was imposed for all analyses and the resulting clusters were corrected for multiple comparisons using Family-Wise Error (FWE)-corrected detection at a threshold of $z > 3.1$, $p < 0.05$. The whole-brain analysis of the localizer tasks allowed us to examine whether semantic control recruits cortical regions fall between DMN and MDN.

Next, to examine whether the task gradient and connectivity gradient captured the organization of semantic networks, we extracted the average connectivity gradient values and task gradient values for matching trials for the voxels falling within each network within participant-specific functional ROIs. These ROIs were defined by selecting the voxels that were most strongly activated for each participant for the relevant localizer contrast (the top 20% of voxels with the highest t-values), within network regions defined at the group level. For DMN, individual subject ROIs were defined using the easy > hard contrast in the spatial working memory and math localizer tasks, within the DMN mask defined at the group level. For both semantic control regions within MDN and MDN regions not implicated in semantic control, individual ROIs were defined using the hard > easy contrast in the spatial working memory and math localizer tasks within the group-level MDN mask defined at the group level. For semantic control regions that fell outside MDN, we identified peak responses to the semantic localizer (words > nonwords) for each participant, within the group word > nonword effect masked by the semantic control network. Within these ROIs, we then extracted the average values on both the task gradient (defined by the parametric effect of semantic similarity during feature matching for each individual) and the principal gradient of connectivity (also defined for individuals using a dimension reduction analysis, as implemented in the BrainSpace toolbox). We then performed repeated-measures ANOVA to test whether there was an orderly change in these values between networks.

2.5.7. Control analysis examining non-matching trials

To examine whether the effects we found for the matching trials were explained by task difficulty, we assessed the parametric effect of global semantic similarity for the non-matching trials (see supplementary materials). We modelled the task gradient by entering the demeaned global semantic similarity ratings for correct non-matching trials as a parametric regressor. For these non-matching trials, global semantic similarity was negatively correlated with accuracy, in contrast to matching trials which showed a positive correlation between global semantic similarity and behavioural performance. Opposite task gradients for matching and non-matching trials would be consistent with these gradients reflecting task difficulty. In contrast, parallel task gradients across matching and non-matching trials cannot be fully explained by task difficulty and might reflect long-term semantic similarity of the inputs. Correlations between the task gradient and connectivity gradient for non-matching trials, together with mixed effects models characterising this relationship, are provided in Supplementary Materials.

2.6. Data and code availability

All summary data, materials and code used in the analysis are accessible in the Open Science Framework at https://osf.io/pa84c/. Raw fMRI data is restricted in accordance with ERC and EU regulations. The conditions of our ethical approval do not permit public archiving of the raw data because participants did not provide sufficient consent. Researchers who wish to access the data should contact the Research Ethics and Governance Committee of the York Neuroimaging Centre, University of York, or the corresponding authors, Xiuyi Wang or Elizabeth Jefferies. Data would be released to researchers when this is possible under the terms of the GDPR (General Data Protection Regulation).

3. Results

3.1. Semantic feature matching performance

Participants saw two words in succession and judged whether they shared a specific feature (colour, shape or size; Fig. 1A). We parametrically varied the global semantic similarity of these two concepts (Fig. 1B), while eliminating concurrent variation with psycholinguistic variables. Global feature similarity ratings for matching trials correlated with both accuracy ($r = 0.35$, $p = 0.000$; Fig. 1C) and response times ($r = -0.22$, $p = 0.007$; Fig. 1D), indicating that participants could more readily judge that items matched on the current goal feature when task-irrelevant characteristics were also shared. For these matching trials, there were no significant correlations between global semantic similarity and word length (number of letters; $r = -0.07$, $p = 0.429$), word frequency (based on SUBTLEX-UK: Subtitle-based word frequencies for British English (van Heuven et al., 2014); $r = 0.05$, $p = 0.586$) or word concreteness (Brysbaert et al., 2014) ($r = 0.07$, $p = 0.394$) of the target word, as shown in Supplementary Figure S1. There was a weak and non-significant correlation between behavioural efficiency and word frequency ($r = 0.14$, $p = 0.092$). There were significant correlations between behavioural efficiency and word concreteness ($r = 0.24$, $p = 0.007$) and word length ($r = -0.19$, $p = 0.024$). However, semantic similarity ratings correlated positively with behavioural efficiency after regressing out word length, word frequency and concreteness ($r = 0.33$, $p < 0.000$), indicating that higher global feature similarity was associated with more efficient feature matching. One third of the trials were 'non-matching' trials, and these also varied from globally semantically-related to unrelated. For these decisions, global similarity hindered rather than aided the decision, leading to poorer accuracy when many features were shared. Further details about the non-matching trials are available in the Supplementary Materials.

3.2. The parametric effect of global semantic overlap

In order to characterise whole-brain spatial patterns relating to the extent to which the presented words were aligned with the structure of long-term semantic knowledge (i.e. the task gradient), we constructed a model that examined the parametric effect of global feature similarity. In this model, demeaned global semantic similarity ratings were included as a parametric regressor. Fig. 3A shows the estimated effect of the parametric manipulation of global feature overlap across the whole brain (i.e., an unthresholded map) for matching trials, when the task-relevant feature was shared between probe and target. (Supplementary Figure S3 shows the main effect of the task; Figure S3 shows the same analysis for non-matching trials in which the task-relevant feature did not match across the probe and target). Positive effects of this variable (i.e., a

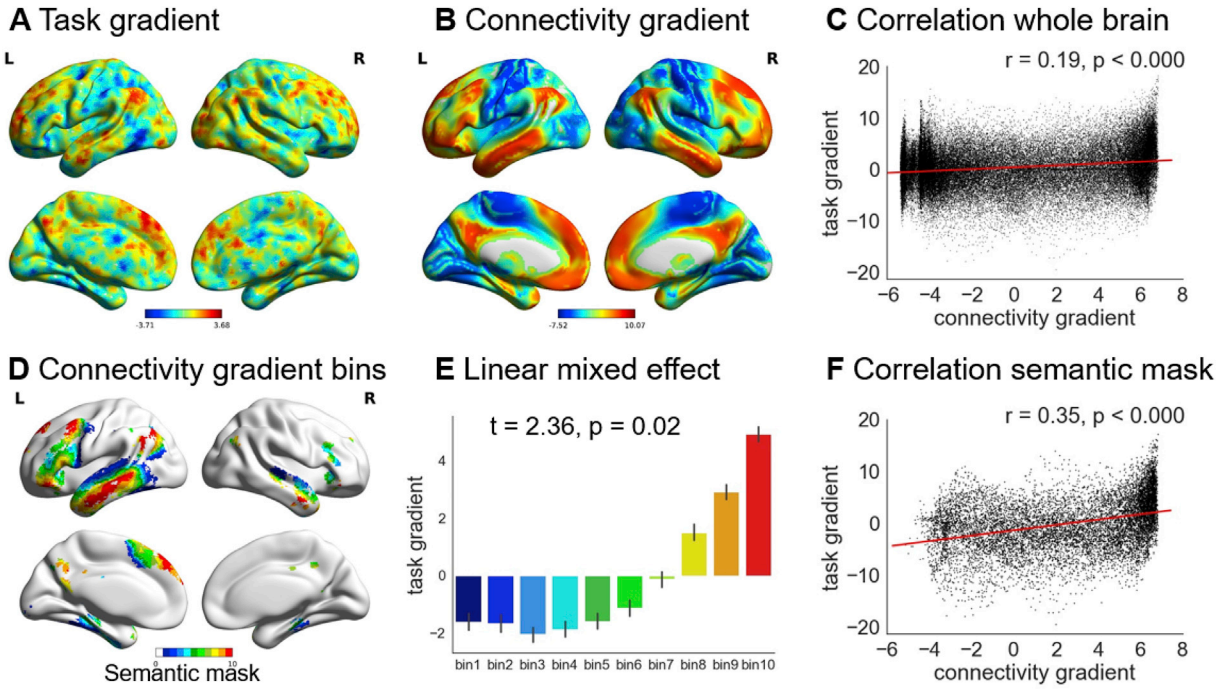

Fig. 3. A – Unthresholded map of the task gradient: i.e. parametric manipulation of global semantic similarity, for trials in which the task-relevant feature was shared across probe and target. Warm colours = positively correlated activity [stronger response when both task relevant and task-irrelevant semantic features were shared between probe and target]. Cool colours = negatively correlated activity [stronger response when only the goal feature was shared between probe and target]. B – The principal gradient of intrinsic connectivity from Margulies et al. (2016). More similar colours reflect brain regions situated at similar points along the principal gradient – i.e. they resemble each other with respect to their patterns of intrinsic connectivity. C – Correlation between the task gradient for matching trials and the connectivity gradient (Margulies et al., 2016) across the whole brain. D – The connectivity gradient (Margulies et al., 2016) within a semantic mask defined using Neurosynth, divided into decile bins according to gradient value: Bin 1 is located towards the unimodal end, while bin 10 is at the heteromodal end of the principal gradient. E – The effect of the task gradient in each bin of the connectivity gradient within the semantic mask, showing that the response to the task changes in an orderly way. F – Correlation between the task gradient for matching trials and the connectivity gradient (Margulies et al., 2016) within the semantic mask defined using Neurosynth.

stronger BOLD response when items share more features) are seen within lateral anterior-to-mid temporal cortex, angular gyrus and medial and superior frontal regions – regions associated with DMN (Raichle, 2015). Negative effects of this variable (i.e., a stronger BOLD response when items share few features) occur in temporal-occipital cortex, intraparietal sulcus, inferior frontal sulcus and pre-supplementary motor area – regions that fall largely in MDN (Duncan, 2010; Fedorenko et al., 2013) (see below for network analysis).

3.3. Correlation between the task gradient for matching trials and the connectivity gradient

Margulies and colleagues found the principal gradient of connectivity (Fig. 3B) was anchored at one end by heteromodal DMN regions, and at the other end by unimodal sensory-motor cortex (Margulies et al., 2016). We found a significant positive correlation between this connectivity gradient and the task gradient (corresponding to the effect of global semantic overlap when the probe and target shared the task-relevant feature). This correlation was significant across the whole brain (Fig. 3C) and was stronger when only voxels associated with semantic processing (falling within a semantic mask from Neurosynth) (Fig. 3D) were included (Fig. 3F). There was a significant difference between these two correlation coefficients ($z = 26.48$, $p < 0.001$), showing that the relationship between the task gradient and the connectivity gradient is to some extent specific to brain regions relevant to semantic processing. The significant correlation exceeded the null distribution based on permutation of the connectivity gradient values (Margulies et al., 2016). The same principal gradient from unimodal sensory-motor cortex to heteromodal DMN regions was revealed using our own resting-state fMRI data, indicated by the high correlation ($r = 0.8$, $p = 0.000$) between our connectivity gradient and the connectivity gradient from Margulies et al. (2016) (Supplementary Figure S6). A similar correlation between the task gradient and connectivity gradient was observed across the whole brain ($r = 0.37$, $p = 0.000$, Supplementary Figure S6). A similar positive correlation between the connectivity gradient and the task gradient was observed for non-matching trials, when the target feature was not shared between the probe and target concepts (Supplementary Figure S3), even though global semantic similarity had the opposite effect on behavioural performance for matching and non-matching trials. This suggests that task difficulty is unlikely to fully account for systematic change in functional recruitment along the connectivity gradient.

Next, to test whether a similar functional organization was present in multiple cortical zones, we calculated the correlation between the connectivity gradient (Margulies et al., 2016) and the task gradient for the matching trials created through our parametric manipulation of global feature overlap. We focused on four anatomically-defined regions: left lateral frontal, left medial frontal, left lateral temporal, and left lateral parietal cortex (see Supplementary Methods), since these sites are extended across the connectivity gradient and they are also broadly implicated in semantic processing (Margulies et al., 2016; Lambon Ralph et al., 2017). We found a significant correlation between the task gradient and the connectivity gradient in all four zones (Fig. 4). The significant correlation exceeded the null distribution based on permutation of the connectivity gradient values (Margulies et al., 2016).

3.4. Systematic change in the effect of the task gradient along the connectivity gradient

To establish if the response to the task gradient for matching trials changed in a systematic way along the connectivity gradient (Margulies et al., 2016) within the semantic mask, we extracted the beta values corresponding to the effect of global semantic similarity within successive bins along the connectivity gradient (Fig. 3D) and examined whether the task response showed a linear change across these bins (Fig. 3E). Since the connectivity gradient varies with physical distance from the DMN (Margulies et al., 2016), a linear trend would suggest that the response to the semantic task changes systematically along the cortical surface. There were ten bins based on deciles, which contained voxels falling within 10% bands along the connectivity gradient, from bin 1 located towards the sensory-motor end of the gradient, through to bin 10 at the heteromodal end overlapping with the DMN (shown in Fig. 3D). We characterised the effect of the task gradient within each bin, for each run and for each participant separately, and performed a linear contrast analysis within a linear mixed effects model, including participant and run as a random effect. There was a linear change along the connectivity gradient in the effect of global feature similarity, indicating an orderly relationship between the task gradient and the connectivity gradient (Margulies et al., 2016). Positive parameter estimates, corresponding to a stronger BOLD response for trials with high global feature similarity in the DMN, gradually reduced in magnitude and became negative at the sensorimotor end of the gradient, reflecting a stronger response for trials with lower global feature similarity ($t = 2.36$, $p = 0.02$, Fig. 3E). None of the higher order effects, such as quadratic and cubic effects, improved the model fit over the linear effect at $p < 0.05$. To test the robustness of the linear effect between the effect of the task manipulation and the connectivity gradient bin, we repeated the analysis using 20 bins along the connectivity gradient and observed the same effects ($t = 2.72$, $p = 0.01$; Supplementary Figure S7). The parameter estimates and further information about the modelling approach are provided in Supplementary Materials.

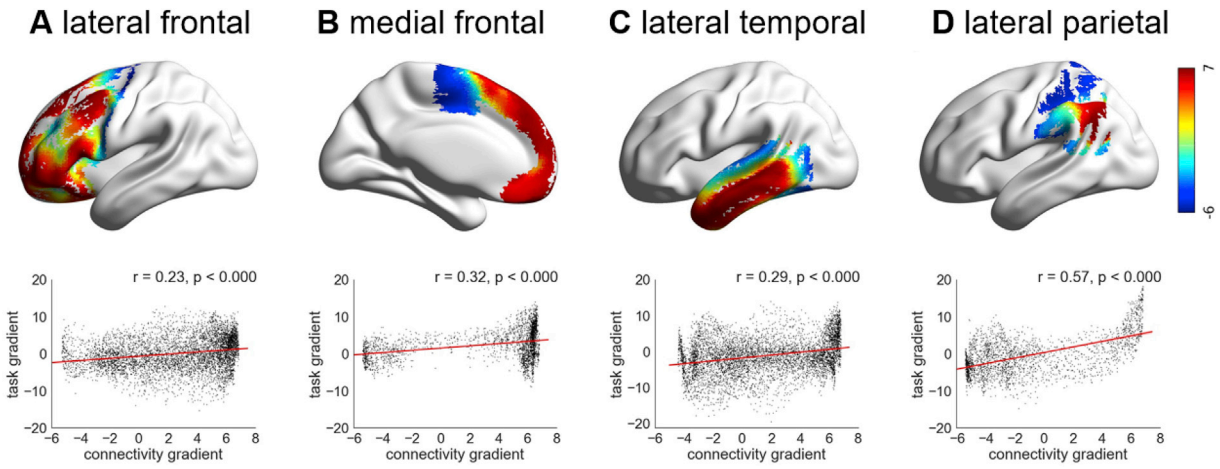

Fig. 4. A, B, C and D show the correlation between task gradient for matching trials and connectivity gradient (Margulies et al., 2016) in lateral frontal, medial frontal, lateral temporal and lateral parietal cortex, respectively. The colour represents each voxel's value on the connectivity gradient defined by Margulies et al. (2016).

3.5. Individuals show the association between the connectivity gradient and task gradient for matching trials

Individual participants are known to show differences in cortical organization which can be obscured at the group level (Braga and Buckner, 2017; Gordon et al., 2017; Laumann et al., 2015; Poldrack, 2017). At the single-subject level, language-selective regions lie adjacent to multiple-demand regions – and, critically, the location of this functional transition is different across individuals (Fedorenko et al., 2012). We therefore examined the voxel-wise correlation between the task gradient for matching trials and the connectivity gradient values (Margulies et al., 2016) in each individual participant. More than half of the participants showed a significant correlation between the connectivity gradient values and effects of global feature similarity across the whole brain (17/30 participants) at $p = 0.05$. The same participants showed correlations that exceeded the null distribution based on permutation of the connectivity gradient values (Margulies et al., 2016). Correlations between connectivity and task gradients were observed in lateral frontal cortex (in 17/30 participants), in medial frontal cortex (in 14/30 participants), in temporal cortex (in 16/30 participants) and in lateral parietal cortex (in 19/30 participants) at $p = 0.05$. Two-thirds of the sample showed a significant correlation between the task and connectivity gradients within the semantic mask generated using Neurosynth (21/30 participants) at $p = 0.05$.

3.6. Semantic control peaks are located at the juxtaposition of DMN and MDN

Although prior studies highlight regions of both DMN and MDN as important in semantic cognition, in situations when the support for semantic decisions from long term memory is minimal, the peak neural response is often observed in regions such as the left inferior frontal gyrus, posterior middle temporal gyrus and dorsal anterior cingulate cortex (Noonan et al., 2013). These peaks typically fall outside the MDN, and are adjacent to, yet distinct from, the DMN (Gonzalez Alam et al., 2018; Humphreys and Lambon Ralph, 2017; Noonan et al., 2013; Wang et al., 2018). Such *semantic control* regions show structural and functional connectivity with regions implicated in long term knowledge (anterior temporal lobes) and domain-general executive control (inferior frontal sulcus) (Davey et al., 2016) and our next analysis considered where these regions are located on both the connectivity gradient observed by Margulies et al. (2016), as well as the task gradient generated by our paradigm. Regions within DMN and MDN were defined in the same participants using non-semantic functional localisers. These were contrasts of easy and hard spatial working memory and math judgements taken from Fedorenko et al. (2011). Consistent with previous findings, DMN regions (showing a stronger response to easy versus hard trials in either task) included posterior cingulate cortex, medial prefrontal cortex, angular gyrus and lateral anterior temporal lobes bilaterally. In contrast, MDN regions (showing a stronger response to hard versus easy trials) included inferior frontal sulcus, premotor cortex, intraparietal sulcus, and lateral occipital cortex (FWE-corrected, $z = 3.1$, $p < 0.05$) (Fig. 5A).

Noonan et al. (2013) found left inferior frontal gyrus, left posterior middle temporal gyrus and dorsal anterior cingulate were the most reliably activated sites across different manipulations of semantic control in a neuroimaging meta-analysis. We compared the location of these semantic control sites with DMN and MDN, as defined by the localizer tasks (Fig. 5A). The semantic control sites overlapped with MDN in lateral and medial prefrontal regions, in line with the view that MDN is recruited whenever task demands are high. However, two of these sites (left inferior frontal gyrus and middle temporal gyrus) also responded to a semantic localizer task, showing stronger activation during the maintenance of strings of words than pronounceable nonwords (FWE-corrected, $z = 3.1$, $p < 0.05$) (Fig. 5B). The word condition was easier than the nonword condition (see Supplementary Materials) and consequently these semantic control regions did not show the functional profile of the MDN. Instead, in left inferior frontal gyrus, left posterior middle temporal gyrus and dorsal anterior cingulate, the response to semantic control demands, defined by Noonan et al. (2013), was observed at the juxtaposition of DMN and MDN. This observation was particularly striking in posterior middle temporal gyrus (Fig. 5A), where the semantic control response was juxtaposed between these two canonical networks.

3.7. The task and connectivity gradients capture the orderly transitions between DMN, semantic control and MDN

To further understand the mapping between the DMN, semantic control and MDN networks, we examined their location along both the task gradient and the connectivity gradient (Margulies et al., 2016). We defined the following cortical regions within the Neurosynth semantic mask: (i) regions within DMN, (ii) semantic control regions from the meta-analysis of Noonan et al. (2013) that fell outside MDN, (iii) semantic control regions within MDN and (iv) MDN regions not implicated

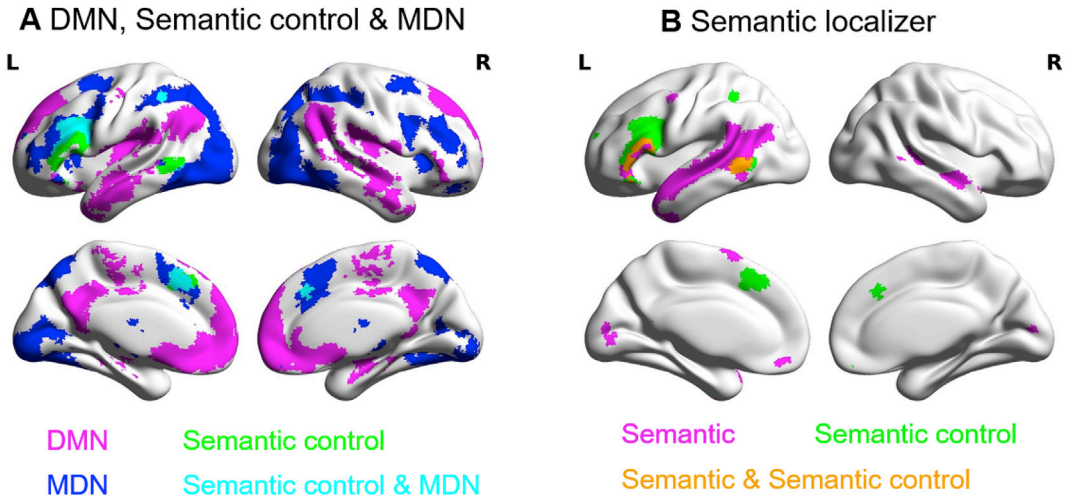

Fig. 5. A – Networks used in the analysis, including DMN (in magenta) and MDN (in blue), defined by the localizer tasks, together with semantic control regions from the meta-analysis of semantic control (Noonan et al., 2013) (in green). B – Semantic regions defined by the semantic localizer task (in magenta), regions implicated in semantic control by an activation likelihood meta-analysis (Noonan et al., 2013) (in green), and their overlap (in orange). This highlights the critical role of left inferior frontal gyrus and posterior middle temporal gyrus in controlled semantic processing.

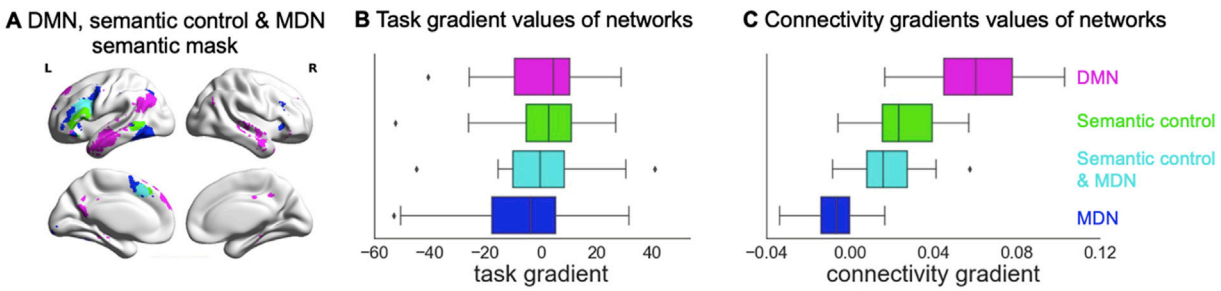

Fig. 6. A – Networks used in the analysis. The same networks shown in Fig. 5A, including DMN, semantic control and MDN, masked by semantically relevant regions, defined using Neurosynth. B – The task gradient values of each network for matching trials. C – The connectivity gradient values of each network.

in semantic control (Fig. 6A). We extracted the average task and connectivity gradient values for the voxels falling within each network, within participant-specific functional ROIs. We were then able to test for significant differences in task and connectivity gradient values between these networks, using the parametric map depicting the effect of varying global semantic similarity during feature matching as well as the principal connectivity gradient map for each participant. We found that task and connectivity gradient values decreased in an orderly fashion across these networks: voxels within DMN had the highest task gradient values, voxels in the semantic control network had lower values, while voxels that fell only in MDN had the lowest values when defining DMN and MDN ROIs using contrasts of easy and hard spatial working memory task (Fig. 6B and C) and math task (provided in Supplementary Materials Figure S8).

Repeated-measures ANOVA was used to examine how task gradient values changed across participants across networks. Mauchly's Test of Sphericity indicated that the assumption of sphericity had been violated ($\chi^2 = 18.001$, $p = 0.003$) and therefore a Greenhouse-Geisser correction was used. There were significant differences in task gradient values across networks ($F(2.175, 60.893) = 4.483$, $p = 0.013$) and a linear trend, capturing the orderly progression in task gradient values from MDN through semantic control to DMN sites ($F(1, 28) = 6.126$, $p = 0.020$). There was no quadratic or cubic trend ($p > 0.05$).

Repeated-measures ANOVA was also used to examine how individually-defined connectivity gradient values changed across participants across networks. We found the same pattern across networks for connectivity gradient values (Fig. 6C). Mauchly's Test of Sphericity again indicated that the assumption of sphericity had been violated ($\chi^2 = 16.344$, $p = 0.006$), and therefore, a Greenhouse-Geisser correction was used. There were significant differences in connectivity gradient values ($F(2.161, 60.512) = 88.066$, $p < 0.000$) and a linear change between networks ($F(1, 28) = 154.882$, $p = 0.000$), capturing an orderly progression in the connectivity gradient from MDN through semantic control to DMN sites. There was also a cubic effect ($F(1, 28) = 16.99$, $p = 0.000$) but no quadratic trend ($p > 0.05$). These findings suggest both the task gradient and connectivity gradient capture the orderly transitions between DMN, semantic control network and MDN.

4. Discussion

Our study investigated the relationship between a large-scale gradient in the organization of the cortex, derived from resting-state connectivity data, and a task-based gradient in BOLD response during a semantic feature-matching task, relating to the strength of association between concepts. We measured neural function using fMRI while participants made decisions about specific conceptual features of words (colour, shape or size), and manipulated the global semantic similarity of the probe and target words parametrically. At one end of this 'task gradient', items shared both goal-relevant and irrelevant features, such that these decisions occurred in a context that was more consistent with unconstrained expectations from long-term memory. At the other end, items had little conceptual overlap beyond those relevant to the goal. Consistent with our hypothesis, we demonstrated that functional recruitment in this task followed the graded organization of the cortex (Margulies et al., 2016): strong global semantic similarity elicited more activation towards heteromodal DMN regions, while weaker global semantic similarity produced more activation within regions linked to executive control and unimodal processing. The association between our task gradient and the connectivity gradient was observed across multiple points on the cortical mantle, and was most clearly seen in regions associated with semantic cognition. This pattern was observed in individual brains, suggesting that it is not a product of group averaging, and it could not be readily explained in terms of task difficulty, since non-matching trials (in which the probe and target concept did not share the task-relevant feature) showed a similar pattern – even though for these items, global semantic similarity was not associated with a behavioural advantage. Finally, we found that the task gradient acts as an organizing principle for the topographical distribution of neural systems implicated in semantic processing, including the observation that the semantic control network falls mid-way between DMN and MDN.

The correspondence between the task gradient and the connectivity gradient: Our study suggests that the organization of the cortex may be optimized to support decision-making across a range of situations that vary from highly familiar to novel. The principal gradient of connectivity is consistent with a hierarchical view of brain organization, in which heteromodal processing emerges from the gradual integration of unimodal sensory-motor representations. This view has been described previously within the temporal lobes by the 'graded hub account' of conceptual representation, which proposes that different modalities (visual, auditory, valence) are gradually integrated within the anterior temporal lobes, with heteromodal conceptual responses falling within ventrolateral regions that are maximally distant from these different inputs (Chiou et al., 2018; Connolly et al., 2018; Lambon Ralph et al., 2017). The whole-brain nature of the principal gradient suggests that a similar gradual abstraction of heteromodal representations occurs across the brain (Guell et al., 2018). Moreover, the principal gradient of connectivity captures the sequence of large-scale networks on the cortical surface, which show orderly transitions from primary visual/-auditory/motor systems, through attention networks, to fronto-parietal control regions, to default mode regions, in multiple zones (Margulies et al., 2016).

We established this macroscale pattern of functional transitions within a single task when decision-making occurred in contexts that varied in their relevance to long-term memory. When many features of the concepts were overlapping, and consequently the presented information was consistent with how we represent information in long-term memory, trials elicited greater engagement at the heteromodal end of the gradient. Conceptual access in both feature-matching and mismatching tasks would be expected to benefit from overlap in long-term conceptual representations towards the DMN-end of the gradient. In contrast, for trials in which only the goal feature was shared by the two concepts, the functional response was maximal further down the gradient, within attentional networks and unimodal regions. In this way our data highlight one important consequence of the pattern of neural

organization described by Margulies et al. (2016): it may reflect how neural organization is optimized to benefit decisions when the structure of long term memory is variably congruent with newly-presented information.

Systematic functional transitions in multiple zones: We found correspondence between the task gradient and the connectivity gradient (Margulies et al., 2016) in multiple cortical zones, including (i) ventral anterior temporal lobe to auditory and visual cortex, (ii) ventromedial to dorsomedial prefrontal cortex, (iii) angular gyrus to intraparietal sulcus, and (iv) inferior frontal gyrus to inferior frontal and precentral sulcus. Although our task involved decisions based on visual features – namely colour, shape and size – functional transitions were observed in regions far from visual cortex. This suggests that the functional gradient is a general principle of whole brain organization that captures multiple local gradients. Our findings are consistent with several local gradients that have been described in isolation (Chiou et al., 2018; Connolly et al., 2018; Guell et al., 2018; Lambon Ralph et al., 2017; Visser et al., 2012). Jackson et al. (2019) identified graded change in the structural and functional connectivity of the ventral medial prefrontal cortex, from DMN to sensory-motor cortex, in line with functional transitions observed in this region (Denny et al., 2012; Sul et al., 2015). Similarly, Badre and D'Esposito (2009) proposed a rostrocaudal gradient in lateral frontal cortex, with rostral frontal areas supporting more abstract forms of control than caudal areas. We observed more complex spatial transitions in lateral frontal cortex, with high gradient values in anterior, ventral and dorsal regions. This is in line with the revised framework of Badre and Nee (2018), which suggests that although the frontal lobes are organized hierarchically, there is no unidimensional spatial gradient of abstraction or global difficulty in this region (Badre and D'Esposito, 2009; Badre and Nee, 2018; Koechlin et al., 2003).

The large-scale task gradient explains the spatial arrangement of networks that support semantic cognition. We found that networks that support semantic cognition are organized in a systematic way along the gradient. Multiple networks with distinct connectivity profiles are recruited in semantic tasks – including DMN regions (such as angular gyrus and lateral middle temporal gyrus) (Humphreys et al., 2015; Wirth et al., 2011), brain regions specifically implicated in semantic control (Noonan et al., 2013), and MDN regions implicated in domain-general executive control (Fedorenko et al., 2013); however, the topographical organization of these networks has not been previously investigated. On both the connectivity and task gradients, the semantic control network had intermediate values – falling in between DMN and MDN in terms of patterns of connectivity and task response. The spatial adjacency of the semantic control network to both DMN and the MDN might allow semantic control regions to integrate long-term conceptual knowledge with more adaptive representations of currently-relevant goals, supporting flexible patterns of semantic retrieval (Davey et al., 2016). This is consistent with recent evidence that DMN and MDN cooperate when memory is controlled (Elton and Gao, 2015; Spreng et al., 2010; Vatansever et al., 2017, 2015).

Graded transitions in the BOLD response from DMN to executive cortex might reflect a shift from intrinsically-guided retrieval based on representations in memory, to a stronger focus on the specific feature information required by the task, when conceptual combinations do not overlap with long-term memory. Across multiple studies, DMN regions show stronger activation when tasks are guided by memory (Humphreys and Lambon Ralph, 2015; Lau et al., 2013; Wirth et al., 2011). In contrast, when current inputs are not a good match with the information in memory, a complementary strategy is needed in which intrinsic cognition is temporarily suppressed. MDN is thought to dynamically alter task processing by coding for information relevant to the current decision (Duncan, 2010) and by changing its pattern of connectivity according to task demands (Cole et al., 2013). Given MDN activates to demanding tasks while DMN typically deactivates (Anticevic et al., 2012), task difficulty might contribute to the functional gradient that we observed for matching trials. However, on non-matching trials (when the probe and target did not share the task-relevant feature), a similar positive correlation was observed between the task gradient and the connectivity gradient – even though global semantic similarity was no longer associated with easier decisions. This suggests that the functional gradient reflects the semantic overlap between probe and target as opposed to cognitive control demands or task difficulty per se.

Further studies that parametrically manipulate other types of semantic and non-semantic tasks are needed to examine the specificity of our findings. A single study cannot fully specify the critical aspects of the task which gave rise to the functional gradient; for example, this research does not address the question of whether the same spatial relationships would be observed for parametric manipulations of non-semantic goals, and/or other semantic tasks, such as global association tasks, that vary in association strength but in the absence of an explicit goal which requires that participants focus on specific features represented at the unimodal end of the gradient. We found that the correlation between the task gradient and the connectivity gradient was maximal within brain regions recruited during semantic tasks, suggesting that if there are similar patterns for non-semantic tasks, these might be strongest in different cortical regions. The unique contribution of the current study is to show that functional recruitment within a task can show systematic variation in a way that follows graded changes in intrinsic connectivity.

5. Conclusions

In summary, we investigated how human cortex is organized to produce a spectrum of cognition, from efficient memory-based decisions to more novel patterns of thought. We developed a paradigm that created a "task gradient" of decisions varying from situations in which there is only weak alignment with semantic information in long-term memory to situations that are strongly anchored by past experience. We found that the brain's response to this task gradient varied systematically with the principal gradient of intrinsic connectivity, with the strongest response in default mode network when the probe and target items were highly overlapping conceptually. This graded functional change was seen in multiple brain regions and within individual brains, and was not readily explained by task difficulty. Moreover, the gradient captured the spatial layout of networks involved in semantic processing, providing an organizational principle for understanding controlled semantic cognition across the cortex.

Declaration of competing interest

The author declare no competing interests.

CRediT authorship contribution statement

Xiuyi Wang: Conceptualization, Investigation, Formal analysis, Writing - review & editing. **Daniel S. Margulies:** Conceptualization, Writing - review & editing. **Jonathan Smallwood:** Conceptualization, Writing - review & editing, Funding acquisition. **Elizabeth Jefferies:** Conceptualization, Writing - review & editing, Funding acquisition.

Acknowledgments

This study was supported by the European Research Council (Project ID: 771863 - FLEXSEM and Project ID: 646927 - WANDERINGMINDS). We are grateful to Evelina Fedorenko for providing us with the localizer tasks and to Evgeny Gluzman for piloting a preliminary version of the task. We thank Deniz Vatansever and Theodoros Karapanagiotidis for suggestions about data analysis.

Appendix A. Supplementary data

Supplementary data to this article can be found online at https://doi.org/10.1016/j.neuroimage.2020.117074.

References

Anticevic, A., Cole, M.W., Murray, J.D., Corlett, P.R., Wang, X.J., Krystal, J.H., 2012. The role of default network deactivation in cognition and disease. Trends Cognit. Sci. https://doi.org/10.1016/j.tics.2012.10.008.

Badre, D., D'Esposito, M., 2009. Is the rostro-caudal axis of the frontal lobe hierarchical? Nat. Rev. Neurosci. 10, 659–669. https://doi.org/10.1038/nrn2667.

Badre, D., Nee, D.E., 2018. Frontal cortex and the hierarchical control of behavior. Trends Cognit. Sci. 22, 170–188. https://doi.org/10.1016/j.tics.2017.11.005.

Badre, D., Wagner, A.D., 2007. Left ventrolateral prefrontal cortex and the cognitive control of memory. Neuropsychologia 45, 2883–2901. https://doi.org/10.1016/J.NEUROPSYCHOLOGIA.2007.06.015.

Behzadi, Y., Restom, K., Liau, J., Liu, T.T., 2007. A component based noise correction method (CompCor) for BOLD and perfusion based fMRI. Neuroimage. https://doi.org/10.1016/j.neuroimage.2007.04.042.

Bemis, D.K., Pylkkänen, L., 2013. Basic linguistic composition recruits the left anterior temporal lobe and left angular gyrus during both listening and reading. Cerebr. Cortex 23, 1859–1873. https://doi.org/10.1093/cercor/bhs170.

Braga, R.M., Buckner, R.L., 2017. Parallel interdigitated distributed networks within the individual estimated by intrinsic functional connectivity. Neuron 95, 457–471. https://doi.org/10.1016/j.neuron.2017.06.038 e5.

Brysbaert, M., Warriner, A.B., Kuperman, V., 2014. Concreteness ratings for 40 thousand generally known English word lemmas. Behav. Res. Methods 46, 904–911. https://doi.org/10.3758/s13428-013-0403-5.

Chiou, R., Humphreys, G.F., Jung, J.Y., Lambon Ralph, M.A., 2018. Controlled semantic cognition relies upon dynamic and flexible interactions between the executive 'semantic control' and hub-and-spoke 'semantic representation' systems. Cortex 103, 100–116. https://doi.org/10.1016/j.cortex.2018.02.018.

Cole, M.W., Reynolds, J.R., Power, J.D., Repovs, G., Anticevic, A., Braver, T.S., 2013. Multi-task connectivity reveals flexible hubs for adaptive task control. Nat. Neurosci. 16, 1348–1355. https://doi.org/10.1038/nn.3470.

Connolly, A.C., Gobbini, M.I., Haxby, J.V., 2018. Three virtues of similarity-based multivariate pattern analysis: an example from the human object vision pathway. Vis. Popul. Codes 1–18. https://doi.org/10.7551/mitpress/8404.003.0016.

Dale, A.M., 1999. Optimal experimental design for event-related fMRI. Hum. Brain Mapp.

Davey, J., Thompson, H.E., Hallam, G., Karapanagiotidis, T., Murphy, C., De Caso, I., Krieger-Redwood, K., Bernhardt, B.C., Smallwood, J., Jefferies, E., 2016. Exploring the role of the posterior middle temporal gyrus in semantic cognition: integration of anterior temporal lobe with executive processes. Neuroimage 137, 165–177. https://doi.org/10.1016/j.neuroimage.2016.05.051.

Denny, B.T., Kober, H., Wager, T.D., Ochsner, K.N., 2012. A meta-analysis of functional neuroimaging studies of self- and other judgments reveals a spatial gradient for mentalizing in medial prefrontal cortex. J. Cognit. Neurosci. 24, 1742–1752. https://doi.org/10.1162/jocn_a_00233.

Duncan, J., 2010. The multiple-demand (MD) system of the primate brain: mental programs for intelligent behaviour. Trends Cognit. Sci. 14, 172–179. https://doi.org/10.1016/j.tics.2010.01.004.

Elton, A., Gao, W., 2015. Task-positive functional connectivity of the default mode network transcends task domain. J. Cognit. Neurosci. 27, 2369–2381. https://doi.org/10.1162/jocn_a_00859.

Fedorenko, E., Behr, M.K., Kanwisher, N., 2011. Functional specificity for high-level linguistic processing in the human brain. Proc. Natl. Acad. Sci. Unit. States Am. 108, 16428–16433. https://doi.org/10.1073/pnas.1112937108.

Fedorenko, E., Duncan, J., Kanwisher, N., 2013. Broad domain generality in focal regions of frontal and parietal cortex. Proc. Natl. Acad. Sci. Unit. States Am. 110, 16616–16621. https://doi.org/10.1073/pnas.1315235110.

Fedorenko, E., Duncan, J., Kanwisher, N., 2012. Language-selective and domain-general regions lie side by side within Broca's area. Curr. Biol. 22, 2059–2062. https://doi.org/10.1016/j.cub.2012.09.011.

Fedorenko, E., Hsieh, P.-J., Nieto-Castañón, A., Whitfield-Gabrieli, S., Kanwisher, N., 2010. New method for fMRI investigations of language: defining ROIs functionally in individual subjects. J. Neurophysiol. 104, 1177–1194. https://doi.org/10.1152/jn.00032.2010.

Fedorenko, E., Scott, T.L., Brunner, P., Coon, W.G., Pritchett, B., Schalk, G., Kanwisher, N., 2016. Neural correlate of the construction of sentence meaning. Proc. Natl. Acad. Sci. Unit. States Am. 113, E6256–E6262. https://doi.org/10.1073/pnas.1612132113.

Gonzalez Alam, T., Murphy, C., Smallwood, J., Jefferies, E., 2018. Meaningful inhibition: exploring the role of meaning and modality in response inhibition. Neuroimage 181, 108–119. https://doi.org/10.1016/j.neuroimage.2018.06.074.

Gordon, E.M., Laumann, T.O., Gilmore, A.W., Newbold, D.J., Greene, D.J., Berg, J.J., Ortega, M., Hoyt-Drazen, C., Gratton, C., Sun, H., Hampton, J.M., Coalson, R.S., Nguyen, A.L., McDermott, K.B., Shimony, J.S., Snyder, A.Z., Schlaggar, B.L., Petersen, S.E., Nelson, S.M., Dosenbach, N.U.F., 2017. Precision functional mapping of individual human brains. Neuron 95, 791–807. https://doi.org/10.1016/j.neuron.2017.07.011 e7.

Guell, X., Schmahmann, J.D., Gabrieli, J.D.E., Ghosh, S.S., 2018. Functional gradients of the cerebellum. Elife 7. https://doi.org/10.7554/eLife.36652.

Humphreys, G.F., Hoffman, P., Visser, M., Binney, R.J., Lambon Ralph, M.A., 2015. Establishing task- and modality-dependent dissociations between the semantic and default mode networks. Proc. Natl. Acad. Sci. U. S. A 112, 7857–7862. https://doi.org/10.1073/pnas.1422760112.

Humphreys, G.F., Lambon Ralph, M.A., 2015. Fusion and fission of cognitive functions in the human parietal cortex. Cerebr. Cortex 25, 3547–3560. https://doi.org/10.1093/cercor/bhu198.

Humphreys, G.F., Ralph, M.A.L., 2017. Mapping domain-selective and counterpointed domain-general higher cognitive functions in the lateral parietal cortex: evidence from fMRI comparisons of difficulty-varying semantic versus visuo-spatial tasks, and functional connectivity analyses. Cerebr. Cortex 27, 4199–4212. https://doi.org/10.1093/cercor/bhx107.

Huntenburg, J.M., Bazin, P.L., Margulies, D.S., 2018. Large-scale gradients in human cortical organization. Trends Cognit. Sci. 22, 21–31. https://doi.org/10.1016/j.tics.2017.11.002.

Jackson, R.L., Bajada, C.J., Ralph, M.A.L., Cloutman, L.L., 2019. The graded change in connectivity across the ventromedial prefrontal cortex reveals distinct subregions. Cerebr. Cortex 1–16. https://doi.org/10.1093/cercor/bhz079, 00.

Jefferies, E., 2013. The neural basis of semantic cognition: converging evidence from neuropsychology, neuroimaging and TMS. Cortex 49, 611–625. https://doi.org/10.1016/j.cortex.2012.10.008.

Kahneman, D., 2003. Maps of bounded rationality: psychology for behavioral economics. Am. Econ. Rev. 93, 1449–1475. https://doi.org/10.1257/000282803322655392.

Karapanagiotidis, T., Vidaurre, D., Quinn, A.J., Vatansever, D., Poerio, G.L., Turnbull, A., Siu, N., Ho, P., Leech, R., Bernhardt, B.C., Jefferies, E., Margulies, D.S., Nichols, T.E., Woolrich, M.W., Smallwood, J., 2019. The psychological correlates of distinct neural states occurring during wakeful rest. bioRxiv 1–15. https://doi.org/10.1101/2019.12.21.885772.

Koechlin, E., Ody, C., Kouneiher, F., 2003. The architecture of cognitive control in the human prefrontal cortex. Science 302 (80), 1181–1185. https://doi.org/10.1126/science.1088545.

Lau, E.F., Gramfort, A., Hämäläinen, M.S., Kuperberg, G.R., 2013. Behavioral/cognitive automatic semantic facilitation in anterior temporal cortex revealed through multimodal neuroimaging. https://doi.org/10.1523/JNEUROSCI.1018-13.2013.

Laumann, T.O., Gordon, E.M., Adeyemo, B., Snyder, A.Z., Joo, S.J., Chen, M.Y., Gilmore, A.W., McDermott, K.B., Nelson, S.M., Dosenbach, N.U.F., Schlaggar, B.L., Mumford, J.A., Poldrack, R.A., Petersen, S.E., 2015. Functional system and areal organization of a highly sampled individual human brain. Neuron 87, 657–670. https://doi.org/10.1016/j.neuron.2015.06.037.

Mahowald, K., Fedorenko, E., 2016. Reliable individual-level neural markers of high-level language processing: a necessary precursor for relating neural variability to behavioral and genetic variability. Neuroimage. https://doi.org/10.1016/j.neuroimage.2016.05.073.

Margulies, D.S., Ghosh, S.S., Goulas, A., Falkiewicz, M., Huntenburg, J.M., Langs, G., Bezgin, G., Eickhoff, S.B., Castellanos, F.X., Petrides, M., Jefferies, E., Smallwood, J., 2016. Situating the default-mode network along a principal gradient of macroscale cortical organization. Proc. Natl. Acad. Sci. Unit. States Am. 113, 12574–12579. https://doi.org/10.1073/pnas.1608282113.

Nee, D.E., D'Esposito, M., 2016. The hierarchical organization of the lateral prefrontal cortex. Elife 5, 1–26. https://doi.org/10.7554/elife.12112.

Noonan, K.A., Jefferies, E., Visser, M., Lambon Ralph, M.A., 2013. Going beyond inferior prefrontal involvement in semantic control: evidence for the additional contribution of dorsal angular gyrus and posterior middle temporal cortex. J. Cognit. Neurosci. 25, 1824–1850. https://doi.org/10.1162/jocn_a_00442.

Peirce, J.W., 2007. PsychoPy—psychophysics software in Python. J. Neurosci. Methods 162, 8–13. https://doi.org/10.1016/j.jneumeth.2006.11.017.

Poldrack, R.A., 2017. Precision neuroscience: dense sampling of individual brains. Neuron 95, 727–729. https://doi.org/10.1016/j.neuron.2017.08.002.

Power, J.D., Barnes, K.A., Snyder, A.Z., Schlaggar, B.L., Petersen, S.E., 2012. Spurious but systematic correlations in functional connectivity MRI networks arise from subject motion. Neuroimage 59, 2142–2154. https://doi.org/10.1016/j.neuroimage.2011.10.018.

Raichle, M.E., 2015. The brain's default mode network. Annu. Rev. Neurosci. 38, 433–447. https://doi.org/10.1146/annurev-neuro-071013-014030.

Ralph, M.A.L., Jefferies, E., Patterson, K., Rogers, T.T., 2017. The neural and computational bases of semantic cognition. Nat. Rev. Neurosci. 18, 42–55. https://doi.org/10.1038/nrn.2016.150.

Schaefer, A., Kong, R., Gordon, E.M., Laumann, T.O., Zuo, X.-N., Holmes, A.J., Eickhoff, S.B., Yeo, B.T.T., 2018. Local-global parcellation of the human cerebral cortex from intrinsic functional connectivity MRI. Cerebr. Cortex 28, 3095–3114. https://doi.org/10.1093/cercor/bhx179.

Snodgrass, J.G., Townsend, J.T., Ashby, F.G., 1985. Stochastic modeling of elementary psychological processes. Am. J. Psychol. https://doi.org/10.2307/1422636.

Spreng, R.N., Stevens, W.D., Chamberlain, J.P., Gilmore, A.W., Schacter, D.L., 2010. Default network activity, coupled with the frontoparietal control network, supports goal-directed cognition. Neuroimage 53, 303–317. https://doi.org/10.1016/j.neuroimage.2010.06.016.

Sul, S., Tobler, P.N., Leiberg, S., Jung, D., Fehr, E., Kim, H., 2015. Spatial gradient in value representation along the medial prefrontal cortex reflects individual differences in prosociality, 112, pp. 7851–7856. https://doi.org/10.1073/pnas.1423895112.

Teige, C., Mollo, G., Millman, R., Savill, N., Smallwood, J., Cornelissen, P.L., Jefferies, E., 2018. Dynamic semantic cognition: characterising coherent and controlled conceptual retrieval through time using magnetoencephalography and chronometric transcranial magnetic stimulation. Cortex 103, 329–349. https://doi.org/10.1016/j.cortex.2018.03.024.

Tversky, A., Kahneman, D., 1974. Judgment under uncertainty: heuristics and biases. Science 185, 1124–1131. https://doi.org/10.1126/science.185.4157.1124.

van Heuven, W.J.B., Mandera, P., Keuleers, E., Brysbaert, M., 2014. Subtlex-UK: a new and improved word frequency database for British English. Q. J. Exp. Psychol. 67, 1176–1190. https://doi.org/10.1080/17470218.2013.850521.

Vatansever, D., Bzdok, D., Wang, H.T., Mollo, G., Sormaz, M., Murphy, C., Karapanagiotidis, T., Smallwood, J., Jefferies, E., 2017. Varieties of semantic cognition revealed through simultaneous decomposition of intrinsic brain

connectivity and behaviour. Neuroimage 158, 1–11. https://doi.org/10.1016/j.neuroimage.2017.06.067.

Vatansever, D., Menon, D.K., Manktelow, A.E., Sahakian, B.J., Stamatakis, E.A., 2015. Default mode network connectivity during task execution. Neuroimage 122, 96–104. https://doi.org/10.1016/j.neuroimage.2015.07.053.

Visser, M., Jefferies, E., Embleton, K.V., Lambon Ralph, M.A., 2012. Both the middle temporal gyrus and the ventral anterior temporal area are crucial for multimodal semantic processing: distortion-corrected fMRI evidence for a double gradient of information convergence in the temporal lobes. J. Cognit. Neurosci. 24, 1766–1778. https://doi.org/10.1162/jocn_a_00244.

Vos de Wael, R., Benkarim, O., Paquola, C., Lariviere, S., Royer, J., Tavakol, S., Xu, T., Hong, S.J., Langs, G., Valk, S., Misic, B., Milham, M., Margulies, D., Smallwood, J., Bernhardt, B.C., 2020. BrainSpace: a toolbox for the analysis of macroscale gradients in neuroimaging and connectomics datasets. Commun. Biol. 3, 1–10. https://doi.org/10.1038/s42003-020-0794-7.

Vos De Wael, R., Larivière, S., Caldairou, B., Hong, S.J., Margulies, D.S., Jefferies, E., Bernasconi, A., Smallwood, J., Bernasconi, N., Bernhardt, B.C., 2018. Anatomical and microstructural determinants of hippocampal subfield functional connectome embedding. Proc. Natl. Acad. Sci. U. S. A 115, 10154–10159. https://doi.org/10.1073/pnas.1803667115.

Wagner, A.D., Paré-Blagoev, E.J., Clark, J., Poldrack, R.A., 2001. Recovering meaning: left prefrontal cortex guides controlled semantic retrieval. Neuron 31, 329–338. https://doi.org/10.1016/S0896-6273(01)00359-2.

Wang, X., Bernhardt, B.C., Karapanagiotidis, T., De Caso, I., Gonzalez Alam, T.R. del J., Cotter, Z., Smallwood, J., Jefferies, E., 2018. The structural basis of semantic control: evidence from individual differences in cortical thickness. Neuroimage 181, 480–489. https://doi.org/10.1016/j.neuroimage.2018.07.044.

Whitfield-Gabrieli, S., Nieto-Castanon, A., 2012. Conn: a functional connectivity toolbox for correlated and anticorrelated brain networks. Brain Connect. 2, 125–141. https://doi.org/10.1089/brain.2012.0073.

Wirth, M., Jann, K., Dierks, T., Federspiel, A., Wiest, R., Horn, H., 2011. Semantic memory involvement in the default mode network: a functional neuroimaging study using independent component analysis. Neuroimage 54, 3057–3066. https://doi.org/10.1016/j.neuroimage.2010.10.039.

Yarkoni, T., Poldrack, R.A., Nichols, T.E., Van Essen, D.C., Wager, T.D., 2011. Large-scale automated synthesis of human functional neuroimaging data. Nat. Methods 8, 665–670. https://doi.org/10.1038/nmeth.1635.